Cancer Letters 412 (2018) 272–282

Contents lists available at ScienceDirect

Cancer Letters

journal homepage: www.elsevier.com/locate/canlet

Original Article

N6L pseudopeptide interferes with nucleophosmin protein-protein interactions and sensitizes leukemic cells to chemotherapy

A. De Cola [a], M. Franceschini [a], A. Di Matteo [b], G. Colotti [b], R. Celani [a], E. Clemente [a], R. Ippoliti [c], A.M. Cimini [c, d, e], A.C. Dhez [c], B. Vallée [f], F. Raineri [f], I. Cascone [f], D. Destouches [f], V. De Laurenzi [a], J. Courty [f], L. Federici [a, *]

[a] Dipartimento di Scienze Mediche, Orali e Biotecnologiche, CESI-MeT, Centro Scienze dell'Invecchiamento e Medicina Traslazionale, Universita' "G. d'Annunzio" Chieti-Pescara, Chieti, Italy
[b] Istituto di Biologia e Patologia Molecolari del CNR, Rome, Italy
[c] Dipartimento di Medicina Clinica, Sanità Pubblica, Scienze della Vita e dell'Ambiente, Università dell'Aquila, L'Aquila, Italy
[d] Sbarro Institute for Cancer Research and Molecular Medicine, Center for Biotechnology, Temple University, Philadelphia, USA
[e] National Institute for Nuclear Physics (INFN), Gran Sasso National Laboratory (LNGS), Assergi, Italy
[f] Universite; Paris-Est Créteil, CNRS, ERL 9215, Laboratoire de Recherche sur la Croissance Cellulaire, la Reparation et la Regeneration Tissulaires (CRRET), Creteil, F-94000, France

ARTICLE INFO

Article history:
Received 1 June 2017
Received in revised form
24 October 2017
Accepted 24 October 2017

Keywords:
NPM1 mutations
Acute myeloid leukemia
Targeted therapy

ABSTRACT

NPM1 is a multifunctional nucleolar protein implicated in several processes such as ribosome maturation and export, DNA damage response and apoptotic response to stress stimuli. The *NPM1* gene is involved in human tumorigenesis and is found mutated in one third of acute myeloid leukemia patients, leading to the aberrant cytoplasmic localization of NPM1. Recent studies indicated that the N6L multivalent pseudopeptide, a synthetic ligand of cell–surface nucleolin, is also able to bind NPM1 with high affinity. N6L inhibits cell growth with different mechanisms and represents a good candidate as a novel anti-cancer drug for a number of malignancies of different histological origin. In this study we investigated whether N6L treatment could drive antitumor effect in acute myeloid leukemia cell lines. We found that N6L binds NPM1 at the N-terminal domain, co-localizes with cytoplasmic, mutated NPM1, and interferes with its protein-protein associations. N6L toxicity appears to be p53 dependent but interestingly, the leukemic cell line harbouring the mutated form of NPM1 is more resistant to treatment, suggesting that NPM1 cytoplasmic delocalization confers protection from p53 activation. Moreover, we show that N6L sensitizes AML cells to doxorubicin and cytarabine treatment. These studies suggest that N6L may be a promising option in combination therapies for acute myeloid leukemia treatment.

Introduction

Nucleophosmin (NPM1) is a nucleolar phosphoprotein expressed in all tissues [1]. It is considered one of the hub proteins of the nucleoli where it plays structural and functional roles through the interaction with several protein and nucleic acid partners [2,3]. NPM1 is involved in several crucial cellular activities including: centrosome duplication [4], rRNA biogenesis and maturation [5], DNA repair [6] and chaperone activity [7]. NPM1 alterations also appear to be involved in cancer development [8,9]. Indeed NPM1 overexpression has been reported in several solid tumors including prostate [10], liver [11], thyroid [12], colon [13], gastric [14], pancreas [15], glioma and glioblastoma [16,17] and often correlates with increased mitotic index and metastasization. The role of NPM1 is also relevant in haematological malignancies where it is often found translocated, deleted or mutated [18]. Notably, *NPM1* is the most frequently mutated gene in AML (acute myeloid leukemia) patients [19,20]. Mutations identified so far are always heterozygous and localized in the terminal exon of the gene [20]. Frameshift insertions cause: the unfolding of the protein C-terminal domain [21]; loss of affinity for nucleic acids [22,23]; loss of the nucleolar localization sequence and the appearance of a new

* Corresponding author. Dipartimento di Scienze Mediche, Orali e Biotecnologiche, CeSI-MeT Centro Scienze dell'Invecchiamento e Medicina Traslazionale, Università di Chieti-Pescara "G d'Annunzio", Via dei Vestini 31, 66100 Chieti, Italy.
E-mail addresses: lfederici@unich.it, luca.federici@unich.it (L. Federici).

https://doi.org/10.1016/j.canlet.2017.10.038
0304-3835/

nuclear export signal [19,24]. As a result, mutated NPM1 is found stably and aberrantly localized in the cytoplasm and it is therefore indicated as NPM1c+. Since the protein heterodimerizes through its N-terminal domain, also wild-type NPM1 is mostly cytoplasmic and only a small fraction of NPM1 is retained in nucleoli in the presence of the mutated form [19,20].

The mechanism by which NPM1c + exerts its tumorigenic activity is not yet completely understood but it has been suggested that the "wrong" cytoplasmic localization may interfere with tumor suppressive mechanisms at multiple levels. For instance NPM1c + interacts with and translocates p14ARF to the cytosol leading to its degradation and thus impairing the p14ARF-HDM2-p53 axis [25]. The same mechanism of delocalization and degradation also applies to the tumor suppressor Fbw7γ, the nucleolar E3-ubiquitin ligase of c-MYC, whose half-life is thus increased in leukemic cells [26]. Furthermore NPM1c + interacts with and inhibits the PTEN deubiquitinating enzyme HAUSP, resulting in PTEN polyubiquitination and degradation [27]. Taken together these studies suggest that moving a critical regulator to the wrong cellular compartment may confer a survival advantage to leukemic cells [28]. These data led us to suggest that new therapeutic strategies aimed at targeting NPM1c + protein-protein associations may be useful for AML treatment [29].

Recently, NPM1 has been identified as one of the targets of the anticancer molecule NucAnt 6L (N6L) [30]. N6L is a synthetic multimeric pseudopeptide, rich in lysine and arginine residues, which has successfully completed phase I/IIa and is currently in preparation for phase II clinical trials. N6L specifically binds a nucleolin-receptor complex overexpressed selectively at the cell surface of tumor cell lines derived from melanoma, glioblastoma, mammary and colorectal carcinoma [30] and, after internalization, mediates anti-tumor activities. N6L inhibits the growth of tumor cell lines, hampers angiogenesis, exerts pro-apoptotic activity *in vitro* and rapidly localizes to tumor tissues *in vivo* [31–36]. N6L has been developed as a nucleolin ligand, however its interaction with NPM1 could be responsible, at least in part, for its anti-tumor activities.

Here we investigated the interaction of N6L with NPM1 and the effect that N6L plays in an AML cell line harbouring NPM1c+, in comparison with an AML cell line where NPM1 is wild-type. We show that N6L interacts with NPM1 N-terminal domain, interferes with NPM1 protein-protein associations and co-localizes in the cytosol with NPM1c+. N6L exerts its toxicity in AML cell lines *via* p53 activation but this effect is strongly delayed in the AML cell line expressing NPM1c+, suggesting that NPM1 delocalization confers resistance to p53 activation. However and importantly, our data also point out that N6L sensitizes AML cells harbouring NPM1c + to both doxorubicin and cytarabine, which are commonly used in AML treatment. Thus, we suggest that the efficacy of N6L may be further explored in combination studies aimed at those AML patients that cannot sustain treatment with either of the two drugs.

Material and methods

SPR analysis

Surface Plasmon Resonance (SPR) experiments were carried out with a SensiQ Pioneer apparatus. Streptavidin-coated BioCap sensorchips were chemically activated by a 35 μl injection of 10 mM NaOH at 10 μl/min flow rate. Biotinylated N6L was immobilized *via* interaction with the streptavidin surface of the chips. The amount of immobilized N6L was detected by mass concentration-dependent changes in the refractive index on the sensor chip surface, and corresponded to about 50 resonance units in each experiment (RU).

Binding experiments were carried out at 298 K in degassed 20 mM HEPES at pH 7.0, 0.15 M NaCl, and 0.005% surfactant P-20 (HBS-P buffer). For both human full-length (FL; residues 16-294) NPM1 and its isolated N-terminal domain (NPM1-Nter; residues 16-123), injections were carried out as follows. The proteins were automatically diluted in HBS-P and injected by 7 serial doubling steps (step contact time = 25 s, nominal flow rate = 100 μl/min), at the following time points: 1) 0–25 s; 2) 26–50 s; 3) 51–75 s; 4) 76–100 s; 5) 101–125 s; 6) 126–150 s; 7) 151–162 s. FL NPM1 concentrations were: 1) 0.375 μM; 2) 0.75 μM; 3) 1.5 μM; 4) 3.0 μM; 5) 6.0 μM; 6) 12 μM; 7) 24 μM and 1) 0.0625 μM; 2) 0.125 μM; 3) 0.25 μM; 4) 0.5 μM; 5) 1.0 μM; 6) 2.0 μM; 7) 4.0 μM; NPM1-Nter concentrations were: 1) 2.34 μM; 2) 4.69 μM; 3) 9.38 μM; 4) 18.75 μM; 5) 37.5 μM; 6) 75 μM; 7) 150 μM and 1) 0.68 μM; 2) 1.55 μM; 3) 3.13 μM; 4) 6.25 μM; 5) 12.5 μM; 6) 25 μM; 7) 50 μM. The increase in RU relative to baseline indicates complex formation between the immobilized N-biotinylated peptide and NPM1 constructs. The plateau region represents the steady-state phase of the interaction. The decrease in RU after 162 s for FL and NPM1-Nter indicates protein dissociation from the immobilized peptide after buffer injection. A response change of 1000 RU typically corresponds to 1 ng/mm^2 change in analyte concentration on the sensor chip. As a negative control, sensor chips were treated as described above in the absence of immobilized N-biotinylated peptides. Values of the plateau signal at steady-state (R_{eq}) and full fittings with 1, 2 and 3 sites were calculated from kinetic evaluation of the sensorgrams using the Qdat 4.0 program.

Fluorescence analysis

Competition experiment was performed at 25 °C in sodium phosphate buffer 20 mM pH 7.2. FluoroMax-4 spectrofluorometer (Jobin Yvon, Edison, NJ, USA), equipped with a water bath apparatus, was used to collect data. NPM1 N-terminal domain and a dansylated peptide of sequence LPFCRRRMKRKLDH, representing the predicted nucleolar localization signal of the Fbw7γ protein (JPT, Germany) were mixed at equal amounts in quantities amenable to ensure complete complex formation (20 μM each). This mixture was titrated with N6L as reported in Fig. 1C. Excitation wavelength was 330 nm and emission spectra were collected in the range between 350 and 650 nm, to monitor dansyl fluorescence.

Cell culture

Acute myeloid leukemia cells (AML-OCI-2 and AML-OCI-3) were grown in MEM-alpha-Medium with high glucose (GibcoBRL). Cell lines were grown in suspension at 37 °C in a humidified atmosphere of 5% (v/v) CO_2 in air. All the media were supplemented with 20% (v/v) fetal bovine serum (FBS) (Euroclone).

Infections

Lentiviruses were produced by transient cotransfection of a three-plasmid expression system in the packaging 293T cells, using the calcium phosphate transfection kit (Invitrogen, Life Technologies). The lentiviral vectors shp53 pLKO.1 puro and scramble shRNA were purchased from Addgene.

Cells were incubated for 7 h with the transfection reagents and viral supernatant was collected 48 h after transfection and filtered through 0.45 μm pore vacuum sterile filtration system (Millipore). Then, AML cells were plated in a six-well plate (Corning) with viral supernatant and 4 μg/mL of polybrene. Plates were centrifuged for 45′ at 1800 rpm and incubated at 37 °C for 75′ in a 5% CO_2 humified chamber. Cells were then washed twice and replated in fresh medium. Cells were selected by puromycin treatment and then infection efficiency was assessed by western blot analysis anti-p53.

Western blotting

Proteins were extracted with a lysis buffer (TRIS-HCl 50 mM pH 8, NaCl 150 mM, Triton X-100 1%, NaF 100 mM, EDTA 1 mM, $MgCl_2$ 1 mM, Glycerol 10%) containing a protease inhibitor cocktail (Sigma-Aldrich) and a phosphatase inhibitor cocktail (Roche). Equal amounts of total protein were subjected to SDS-PAGE and then electrotransferred to nitrocellulose membranes. The membranes were blocked with 5% nonfat dry milk in PBS with 0,1% Tween 20 and incubated over-night using the following antibodies: anti β-Actin A5441 (Sigma), anti-NPM1, anti-Fibrillarin, anti-p14 ARF (Cell Signaling), anti-p21 and anti-p53 (Santa Cruz), anti-Nucleolin (Upstate, Millipore) anti-NPM1 Thr199 and Thr234/237 (Biolegend). After wash, membranes were hybridized with horseradish peroxidase-conjugated secondary antibodies (rabbit and mouse, Biorad, CA, USA). Detection was performed with Plus-ECL chemiluminescence kit (PerkinElmer, Inc.; MA, USA) or with SuperSignal West Dura extended duration substrate kit (Thermo Scientific, USA).

In vitro apoptosis assays

Apoptotic cell death in the presence of 20 μM N6L for 24 h and 48 h was evaluated by Annexin V staining. Briefly cells were resuspended in Annexin V binding buffer containing allophycocyanin (APC)-labeled Annexin V (BD Biosciences) and 7-Amino-Actinomycin D (7-AAD) as a viability probe. A FACSCantoII flow cytometer, running with FACSDiVa software (BD Biosciences), was used for sample acquisition and analysis.

Caspase-3/7 activity was measured using the Caspase-Glo 3/7 detection assay kit according to the manufacturer's instruction (Promega) with Synergy H1 Gen5 microplate reader and Imager (Biotek).

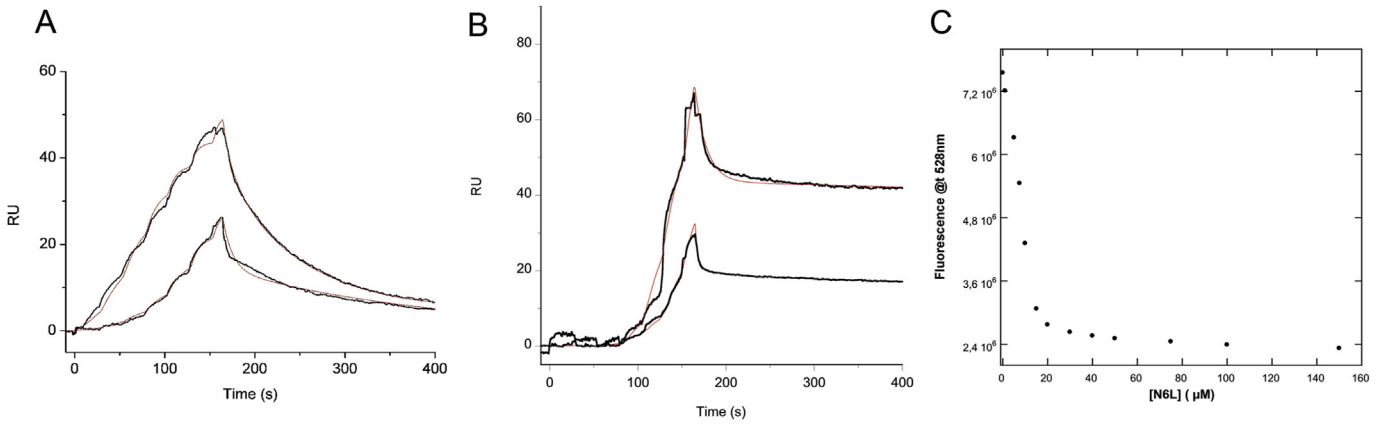

Fig. 1. Interaction between N6L and NPM1. (**A**) SPR measurement of the interaction between immobilized biotynilated N6L and full-length NPM1. Protein was automatically diluted in HBS-P and injected by 7 serial doubling steps (step contact time = 25 s, nominal flow rate = 100 μl/min). At the following time points: 1) 0–25s; 2) 26–50s; 3) 51–75s; 4) 76–100s; 5) 101–125s; 6) 126–150s; 7) 151–162s. NPM1 concentrations were: 1) 0.375 μM; 2) 0.75 μM; 3) 1.5 μM; 4) 3.0 μM; 5) 6.0 μM; 6) 12 μM; 7) 24 μM (upper trace and 1) 0.0625 μM; 2) 0.125 μM; 3) 0.25 μM; 4) 0.5 μM; 5) 1.0 μM; 6) 2.0 μM; 7) 4.0 μM lower trace. Experimental data were fitted according to a three-site binding model (red trace). (**B**) SPR measurement of the interaction between immobilized biotynilated N6L and NPM1-Nter under the same setting of panel A. NPM1-Nter concentrations were: 1) 2.34 μM; 2) 4.69 μM; 3) 9.38 μM; 4) 18.75 μM; 5) 37.5 μM; 6) 75 μM; 7) 150 μM. Data were according to a two-site binding model (red trace). (**C**) Displacement of Fbw7γ NoLS peptide by N6L. NPM1-Nter and dansylated Fbw7γ NoLS peptide were mixed at equal amounts (20 μM) and fluorescence intensity was titrated with increasing amounts of N6L as reported. (For interpretation of the references to colour in this figure legend, the reader is referred to the web version of this article.)

Cell proliferation assay

AML cells were seeded into 12-well plate at 2×10^5 cells/well. Viable cell count was performed with Trypan Blue reagent (Sigma-Aldrich) at the indicated time points. When indicated, cells were treated with 5, 10, 20 μM N6L, 40 μM ARA-C, 0,5 μM doxorubicin.

For time course and dose dependence experiment, AML cells were seeded into 96-well plate at 2000 cells/well treated or not with 20, 40, 60, 80 μM N6L for 24, 48, 72 and 96 h. Cell viability was evaluated with CellTiter-Blue Cell Viability Assay according to the manufacturer's instruction (Promega) and measured with Synergy H1 Gen5 microplate reader and Imager (Biotek).

Immunofluorescence

OCI-AML2 and OCI-AML3 cells were spotted on microscope slides with cytospin and then were fixed in 4% (wt/vol) paraformaldehyde in PBS for 10 min. After fixation they were permeabilized with 0.1% Triton X-100 for 10 min and then incubated for 1 h in 10% goat serum. After blocking, cells were incubated over night with rabbit anti-NPM antibody (1:50 dilution, Cell Signaling Technology), and with mouse anti-Nucleolin antibody (1:100, Upstate Millipore, Lake Placid, NY) in blocking solution. Cells were washed for three times and incubated for 1 h with secondary antibodies: goat anti-rabbit-Alexa 488; goat anti-mouse-Alexa 568 (Molecular Probes, Eugene, OR, USA) and when indicated with N6L-alexa fluor 488 0.5 μM in blocking solution. Then, cells were washed twice and nuclei were stained with DRAQ5 for 30 min and fixed with Prolong Gold antifade kit (Molecular Probes, Invitrogen). Confocal imaging was performed using a microscope LSM 510 META (Carl Zeiss, Germany) and analysed with Zen software from Zeiss.

FACS analysis

OCI-AML2 and OCI-AML3 cells were seeded into 96-well plate at 2×10^5/well and 1 μM N6L Alexa 488 was added for 2 h at 37 °C, 5% CO2. After washing with PBS cells were resuspended in PBS and 7-Amino-Actinomycin D (7-AAD) was added as a viability probe. Cytofluorometry data were acquired by MACSQuant® Analyzer 10 for at least 10.000 cells and analysed by MACSQuantify™ Software.

For nucleolin staining, 1×10^5 OCI-AML2 and OCI-AML3 living cells were collected and incubated on ice for 30 min with mouse anti-nucleolin antibody (1:100, Upstate Millipore, Lake Placid, NY). After wash in PBS, cells were incubated for 20 min on ice with secondary antibody goat anti-mouse-Alexa Fluor 488 (1:300, Molecular Probes, Eugene, OR, USA). Then cells were washed twice and data were acquired by FACSCantoII flow cytometer, running with FACSDiVa software (BD Biosciences).

Results

Analysis of the interaction between N6L and NPM1

Previous studies suggested that N6L binds NPM1 with high affinity [30]. In order to confirm these data and get further insight into the binding mechanism we used Surface Plasmon Resonance analysis and biotinylated N6L immobilized into a streptavidin chip as a ligand. Fig. 1A reports the binding experiment performed using full-length NPM1 (aa 16-294) as the analyte. Multiple consecutive injections of NPM1, from 0.375 to 24 μM for the upper trace, and from 0.0625 to 4.0 μM for the lower trace, were performed. NPM1 was then let to dissociate by buffer injection and the dissociation phase was followed until completion. Data were globally fitted using different binding models. We found that the best fit was obtained with a three-site model, which yielded two high affinity sites, with dissociation constants in the nanomolar range, and one lower affinity site (Table 1). To get further insight into the regions of the proteins involved in N6L recognition, we also measured the binding of NPM1 N-terminal domain (NPM1-Nter; residues 16-123) to immobilized N6L. Fig. 1B shows the traces obtained by injecting NPM1-Nter in the 2.34–150 μM and in the 0.68–50 μM concentration ranges. In this case, data were best fitted using a two-site model, one with nanomolar affinity and the other with lower micromolar affinity (Table 1). Taken together, these data suggest that N6L readily recognizes NPM1-Nter but that at least one additional high-affinity binding site is present in the full-length protein.

NPM1-Nter has been recently recognized as the site for the majority of NPM1 protein-protein interactions [37,38]. In particular, we have shown that NPM1-Nter binds the nucleolar localization signal (NoLS) in its protein partners, thus contributing to their nucleolar localization [38]. The NoLS consists of a linear stretch of amino acids enriched in positively charged residues [39], which are recognized by a wide negatively charged area at the external surface of the NPM1-Nter pentamer [38]. Since N6L is also enriched in positively charged residues, we hypothesized that it might bind the same region of NPM1-Nter that recognizes the NoLS in its protein

Table 1
Dissociation constants for the interaction between N6L and NPM1 constructs.

		K_D
FL NPM1	Site 1	99 ± 10 nM
	Site 2	470 ± 38 nM
	Site 3	4.3 ± 0.3 μM
Nter NPM1	Site 1	149 ± 22 nM
	Site 2	244 ± 28 μM

partners. In order to test this, we set up a displacement experiment where the complex between NPM1-Nter and the NoLS peptide from Fbw7γ, dansylated at its N-terminus, was titrated with increasing amounts of N6L. Fig. 1C shows the decrease of dansyl fluorescence as a function of N6L concentration, which indicates that N6L binds NPM1-Nter and, in doing so, effectively displaces the Fbw7γ NoLS peptide from NPM1-Nter. This experiment demonstrates that N6L interferes with NPM1 protein-protein associations.

In order to investigate the effect of N6L on the nucleolar structure and localization of NPM1 and nucleolin, we used OCI-AML2 cells, which carry wild-type NPM1 at both alleles, and OCI-AML3 cells, carrying heterozygous NPM1 mutation type A and expressing NPM1c+ [40]. Cells were treated with 20 μM of N6L for 24 h. Immunofluorescence analysis (Fig. 2A and B) shows that NPM1 and nucleolin retain their localization upon treatment, in both cell lines. As to NPM1, this is consistent with N6L not interacting with the C-terminal domain of the protein, which mediates nucleic acids binding and nucleolar localization [41,42].

FACS analysis was used to evaluate the amount of N6L incorporated in both cell lines and it was observed that the total uptake of N6L is higher in OCI-AML2 than in OCI-AML3 cells (Fig. 2C). It has been shown that a main mechanism for N6L entry into cells consists in its recognition by cell surface nucleolin expression [30,31]. Therefore, in order to address the different rate of N6L uptake between the two cell lines, we checked cell surface nucleolin expression. As shown in Fig. S1, FACS analysis indicates that nucleolin is present at the surface of both cell lines but at very low and not statistically significant levels. Therefore we cannot exclude that other mechanisms for N6L entry take place in our leukemic cell models and are responsible for the increased efficiency in OCI-AML2 cells. We also studied N6L cell localization and trafficking using N6L-AlexaFluor488 in conjunction with anti-NPM1 and anti-nucleolin antibodies. As shown in Fig. 2D, N6L mostly accumulates in the nucleoli of OCI-AML2 cells where it colocalizes with NPM1 and nucleolin. This indicates that, as in other types of cancer, N6L translocates from the cell surface to the nucleoli and suggests that NPM1 and nucleolin may be involved in N6L trafficking and nucleolar retention. Importantly, Fig. 2D shows that a consistent fraction of N6L is retained in the cytosol of OCI-AML3 cells, where it colocalizes with cytosolic NPM1c+ (Fig. 2D). The observation that N6L enters AML cells, with and without NPM1 mutation, prompted us to further investigate the effect of N6L in these cell lines.

N6L induces p53 dependent cell death

We then tested the effect of N6L on AML cells viability and cell death. As shown in Fig. 3A and B, treatment with N6L resulted in reduced viability and a dose dependent death in OCI-AML2 cells. Interestingly, despite the previously observed cytosolic interaction with NPM1c+, OCI-AML3 cells appear to be substantially less sensitive to N6L treatment. Moreover, due to the higher uptake of N6L in OCI-AML2 cells, we also performed a dose response and time course cell viability assay treating AML cells with 20, 40, 60 and 80 μM of N6L from 24 to 96 h. Fig. 3C demonstrates that even when N6L reach higher intracellular levels in OCI-AML3 cells, these are still more resistant. Specifically, using a 4-fold higher dose of N6L in OCI-AML3 cells (80 μM) does not reduce cell viability as compared to the lower dose used for OCI-AML2 cells (20 μM).

To further characterize N6L-induced cell death, we also quantified apoptosis by Annexin V/7-AAD staining. As shown in Fig. 4A, N6L markedly increased OCI-AML2 cell apoptosis in a dose-dependent and time-dependent manner, while this effect was negligible in OCI-AML3 cells. We also performed a Caspase 3/7 enzymatic assay, further confirming activation of a classic caspase dependent apoptotic pathway in OCI-AML2 cells while, once again, this effect was only slightly appreciable and only at the highest dose in OCI-AML3 cells (Fig. 4B).

Next we investigated whether N6L toxicity is mediated by the activation of the p53 pathway. As shown in Fig. 4C, treatment with N6L resulted in a dose dependent increase of p53 protein levels in both cell lines that are paralleled by increased levels of p21 and p14ARF, two well known p53 targets. Notably, however, levels of p53, p21 and p14ARF are reduced in OCI-AML3 cells with respect to OCI-AML2, both before and after N6L treatment, at all dosages. In order to assess the effect of N6L on nucleolar structure, we also analysed the levels of NPM1 and two other nucleolar marker proteins, known to interact with NPM1: nucleolin and fibrillarin. The former is also known to bind N6L. Interestingly, treatment with N6L leads to NPM1, nucleolin and fibrillarin decreased levels, in a dose dependent manner, in OCI-AML2 cells. This effect is also observed in OCI-AML3 cells but to a lesser extent (Fig. 4C).

We have previously shown that N6L treatment induces a reduction of NPM1 phosphorylation at residue Thr199 without affecting its expression in prostate cancer [35]. Therefore we also investigated the effect of N6L on the Thr199-phosphorylated form of NPM1. As shown in Fig. 4D, treatment with N6L induced a dose-dependent decrease in the expression of both NPM1 and its Thr199-phosphorylated form in OCI-AML2 and to a lesser extent in OCI-AML3 cells.

To confirm that N6L induced death is indeed p53 dependent, we silenced this gene in both AML cell lines with a lentiviral shp53 constructs or a scrambled control (Fig. 5A) and we treated them with 20 μM of N6L. As shown in Fig. 5B and C, silencing of p53 almost completely abrogates N6L induced death in OCI-AML2 cells. As expected no effect is seen in the already resistant OCI-AML3 cells. We also analysed the expression levels of the p53 target gene p21 under this setting. Fig. 5D shows that, in p53 silencing conditions, there is no consistent increase of p21 in response to N6L treatment, confirming that N6L-induced cell death proceeds through the activation of the p53 axis.

N6L sensitizes leukemic cells to doxorubicin and cytarabine treatment

The results we obtained so far demonstrate that N6L has apoptotic activity *in vitro* on OCI-AML2 cells, bearing the WT form of NPM1. Conversely, this effect is negligible on OCI-AML3 cells, expressing NPM1c+. Thus, given the low success of N6L used as a single agent on OCI-AML3 cells, we wondered whether N6L could have a synergic effect on standard anthracycline and cytarabine-based anti-leukemia chemotherapy. To assess this issue, we first treated OCI-AML2 and OCI-AML3 cells with doxorubicin from 0,1 to 1–3 μM in combination or not with N6L (20 μM) for 24 h. Fig. 6A shows that N6L co-treatment displays an additive effect on OCI-AML2 cells at all doxorubicin dosages. Interestingly, OCI-AML3 cells are also more resistant to doxorubicin treatment than OCI-AML2 cells. However, and importantly, N6L co-treatment resulted in significantly increased sensitivity of OCI-AML3 cells, when these were treated with the higher doxorubicin dosage of 3 μM (Fig. 6A, right panel).

Then we also tested the effect of cytarabine (ARA-C) on our leukemic cell models, treating them initially with concentrations ranging from 1 to 3 μM. Results indicate that OCI-AML2 are sensitive to cytarabine and that N6L significantly enhances this effect (Fig. 6B left panel); conversely OCI-AML3 cells are resistant to these ARA-C doses and its concentration had to be raised up to 40 μM to obtain a consistent cell death (Fig. 6B, right panel). To highlight possible synergic effects of N6L and ARA-C combined treatment we also extended our assay to 48 h. Data in Fig. 6C show that the combined treatment with both drugs significantly enhanced cell

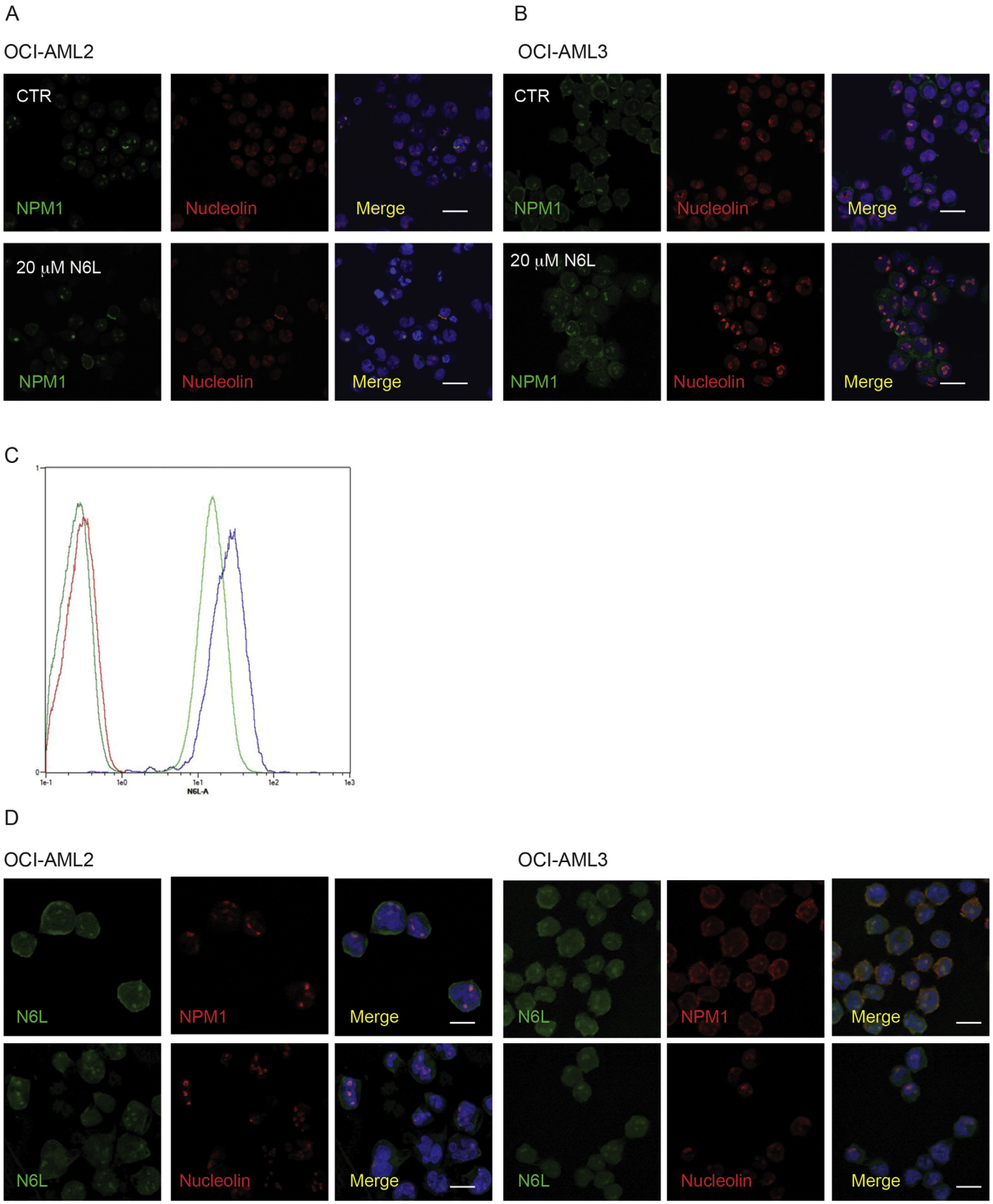

Fig. 2. Immunofluorescence of OCI-AML2 **(A)** and OCI-AML3 **(B)** cells treated or not with 20 μM N6L for 24 h and stained with anti-Nucleophosmin antibody (NPM-1, green) anti-Nucleolin antibody (red) and with DRAQ5 dye to highlight the nucleus (scale bar: 20 μm). (**C**) The uptake of N6L in OCI-AML3 cells (green line) is estimated to be reduced by 65% with respect to OCI-AML2 cells (blu line) (n = 2). The uptake of 1 μM N6L AlexaFluor −488 after 2 h of incubation was analysed by FACS in live cells; dead cells were excluded by using the death dye 7AAD. (**D**) N6L internalization by AlexaFluor-488 N6L (green) and colocalization with NPM1 and Nucleolin (red) in OCI-AML2 and OCI-AML3 cells (scale bar: 10 μm). (For interpretation of the references to colour in this figure legend, the reader is referred to the web version of this article.)

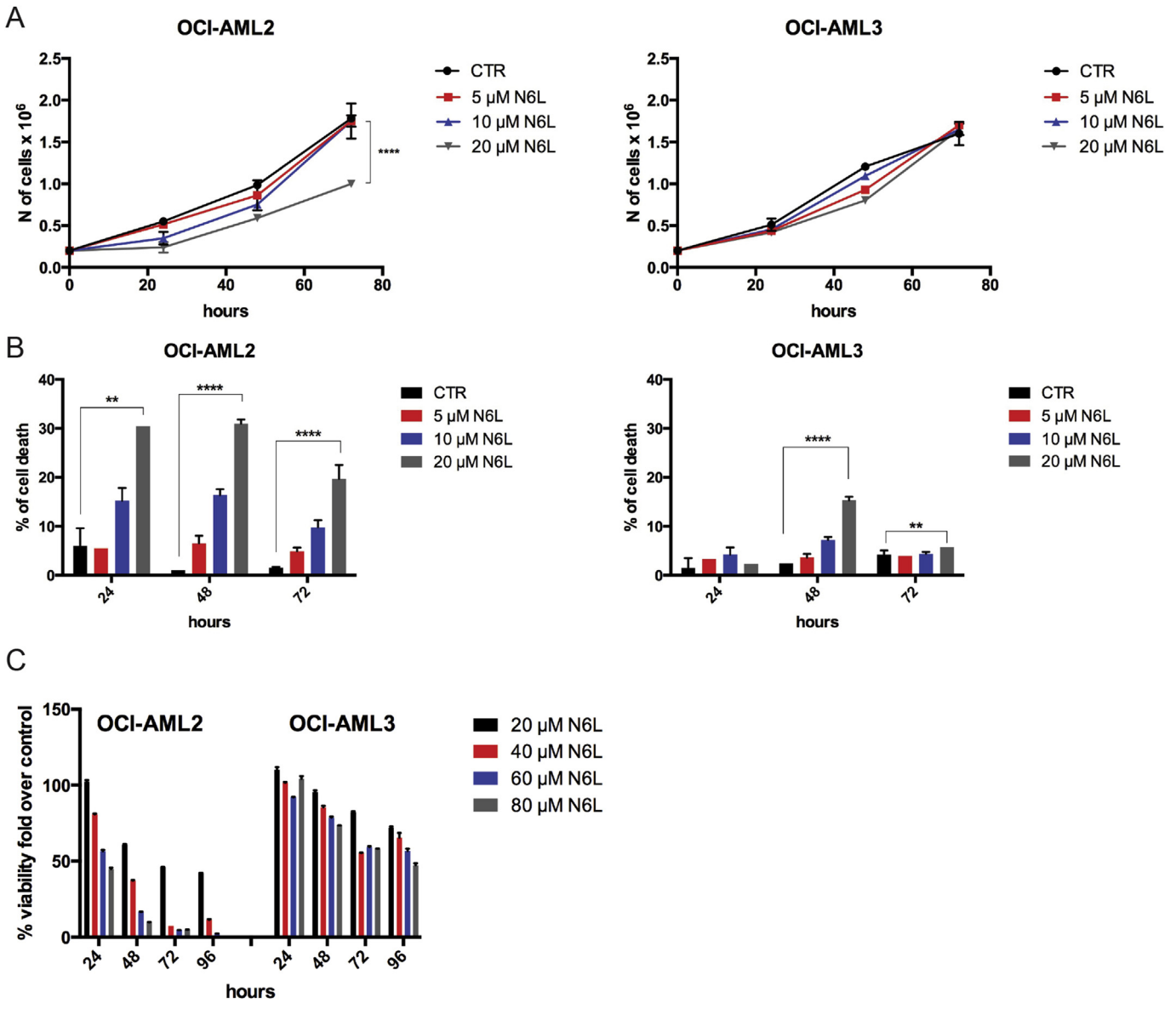

Fig. 3. (**A**) Cell proliferation assay of OCI-AML2 and OCI-AML3 untreated (ctr) or treated with 5, 10 and 20 μM of N6L at the indicated time points (hours). Data represent mean ± SD of five different experiments, each performed in duplicate, analysed with Anova test with a p value **** < 0,0001. (**B**) Percentage of OCI-AML2 and OCI-AML3 cell death after treatment as described above; p values by Anova test are shown in the graph (p **** < 0,0001 and p ** < 0,002). (**C**) Percentage of fold over control OCI-AML2 and OCI-AML3 viability after treatment with 20, 40, 60 and 80 μM N6L at the indicated time points (hours).

death with respect to both N6L and ARA-C alone, both at 24 h and 48 h.

Finally we also tested the combined treatment with all three compounds and in Fig. 6D we report a comprehensive view of the effects obtained on cell viability and cell death. The addition of N6L, as a third drug, to the combination of doxorubicin and ARA-C resulted in only a modest increase in toxicity (Fig. 6D). However it also shows that the doxorubicin-N6L combination is as effective as the doxorubicin-ARA-C one, and more effective than doxorubicin alone.

Discussion

NPM1 mutations are the most frequent genetic alteration in AML and their hallmark is the aberrant accumulation of NPM1 in the cytosol of leukemic blasts, both mutated and wild-type [19,20]. They consist in frameshift insertions in the terminal part of the gene that turn the nucleolar localization signal of the protein into a newly formed nuclear export signal. From the structural point of view, mutations cause the unfolding of the C-terminal three-helix bundle domain [24,43], resulting in loss of affinity for nucleoli because of impaired nucleic acid binding [22,23]. Given that wild-type NPM1 is able to oligomerize with NPM1c+, also the majority of the former is delocalized in the cytoplasm while only a minor but still detectable fraction is retained in nucleoli.

NPM1 mutations are always exclusive of other recurrent genetic abnormalities, always retained at relapse and characterized by distinctive gene expression and microRNA profiles [28]. These and other observations have led to the suggestion that they are founder mutations in AML and therefore that NPM1c + should be specifically targeted in this kind of leukemia [28]. Under this light, since the discovery of NPM1 mutations in 2005 [19], a great deal of research has highlighted several gain of function activities played by NPM1c+ in the cytosol, that provide a survival advantage to

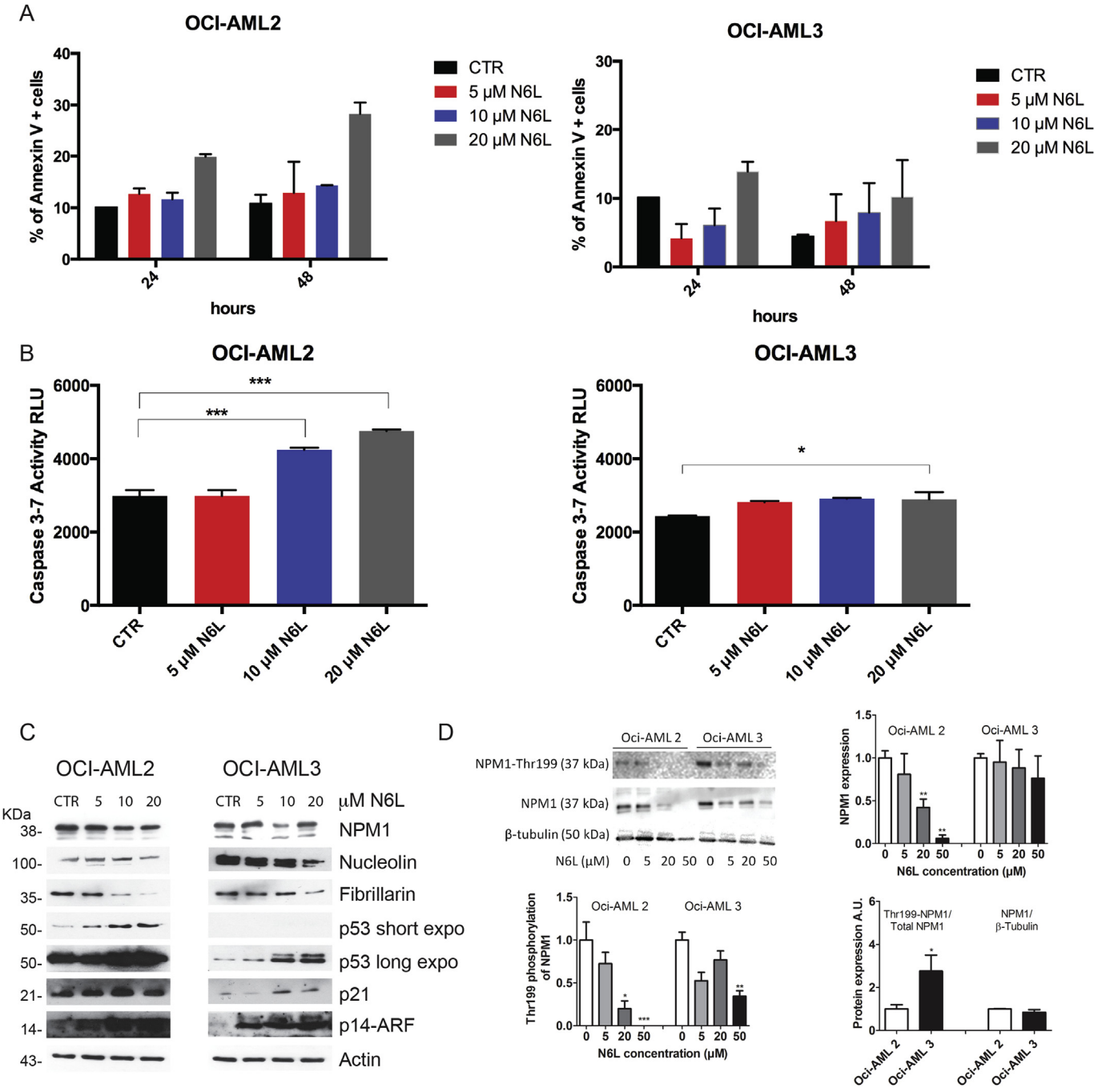

Fig. 4. (**A**) Flow cytometry percentage of apoptotic OCI-AML2 and OCI-AML3 positive cells stained by Annexin V measured after 24 and 48 h of 20 μM N6L treatment. (**B**) Caspase 3–7 activity of OCI-AML2 and OCI-AML3 cells treated for 24 h with different N6L concentrations; RLU relative light units. Data were analysed with Anova test with ***p value = 0,0002 and *p value = 0,02. (**C**) Western blot analysis of NPM1, Nucleolin, Fibrillarin, p53, p21 and p14-ARF expression levels upon N6L treatment for 24 h at the indicated doses. Actin was used as a loading control. (**D**) Western blot analysis of NPM1 and its Thr199 phosphorylated form expression levels, upon N6L treatment for 72 h at the indicated doses. β-tubulin was used as a loading control. The experiment has been performed in triplicate. The expression levels of NPM1 and its phosphorylated form in the two cell lines upon N6L treatment were quantified by densitometry using ImageJ software. The NPM1 expression was normalized with the β-tubulin expression and Thr199 phosphorylated NPM1 with the total NPM1 expression.

leukemic blasts. Among them we enlist the cytosolic displacement and degradation of p14ARF [25] and Fbw7γ [26], the interaction with HAUSP [27] and with caspases 6 and 8 [44] and others. It should be emphasized that most of these unwanted activities are due to interactions that NPM1c + plays with other proteins. For this reason, we have recently suggested that an effective strategy to target NPM1 in this type of leukemia would be to interfere with its protein-protein associations [29]. Recently, we have investigated the structural basis of NPM1 protein-protein interactions [38] showing that NPM1-Nter is able to interact with a vast number of proteins by recognizing their NoLSs, which consist in linear stretches of amino acids enriched in positively charged residues, with its N-terminal domain.

N6L is a synthetic pseudopeptide originally designed to interact with cell surface nucleolin but recently shown to also interact with NPM1 [30]. Since N6L is enriched in positively charged residues, we

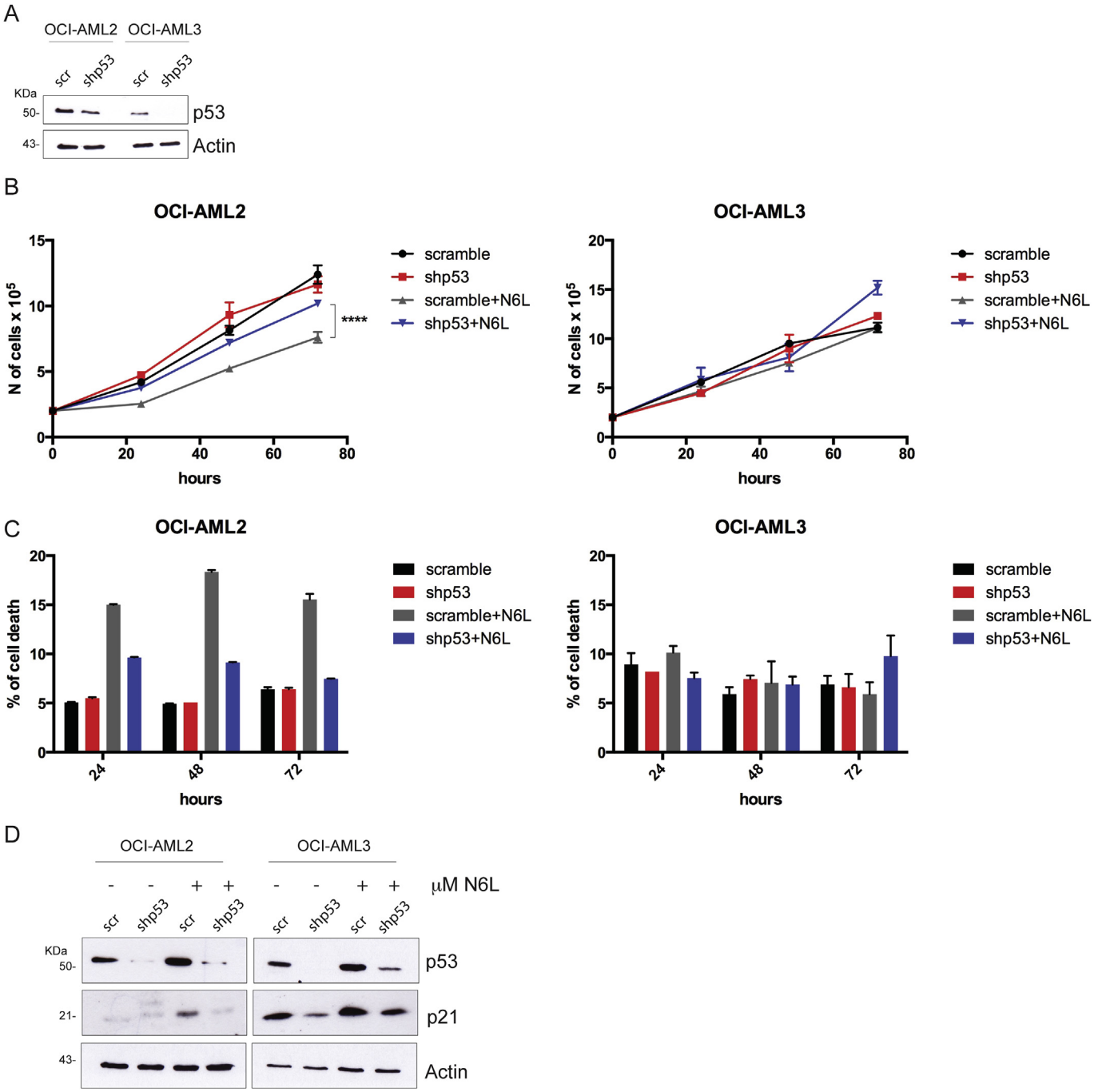

Fig. 5. (**A**) Western blot analysis of p53 protein levels in OCI-AML2 and OCI-AML3 infected with p53 silencing lentivector (shp53) or with a scramble control (ctr). Actin was used as a loading control (**B**) Cell proliferation assay of OCI-AML2 and OCI-AML3 cells infected with p53 silencing lentivector (shp53) or with a scramble control (ctr), treated or not with 20 μM of N6L for 24, 48 and 72 h. (**C**) Percentage of OCI-AML2 and OCI-AML3 cell death after treatment as described above. Data represent mean ± SD of three different experiments, each performed in duplicate, analysed with Anova test with a p value **** < 0,0001. (**D**) Western blot analysis of p53 and p21 expression levels of OCI-AML2 and OCI-AML3 infected with p53 silencing lentivector (shp53) or with a scramble control (ctr), treated or not with 20 μM of N6L for 72 h.

argued that it might also interact with NPM1-Nter. Indeed, we show here that this is the case with at least one high affinity binding site and a much lower affinity one. In addition, data collected with the full-length protein suggest the presence of an additional high-affinity binding site. Even if the exact position of this binding site has to be determined, we hypothesize that it might be located at the protein's central domain, where a linear stretch of more than 20 negatively charged residues is present. Finally and importantly we also show that N6L binds NPM1-Nter at the same site of protein partners' NoLS and that effectively interferes with NPM1 protein-protein associations.

These results suggest that N6L might be used as an investigational drug to test the idea of interfering with NPM1 protein-protein associations in AML. To this purpose we used AML cells harbouring the WT NPM1 gene (OCI-AML2 cells) or the mutated form (NPMc+; OCI-AML3 cells). We found that N6L is internalized in both OCI-AML2 and OCI-AML3 cells, even though a higher uptake was observed in the former.

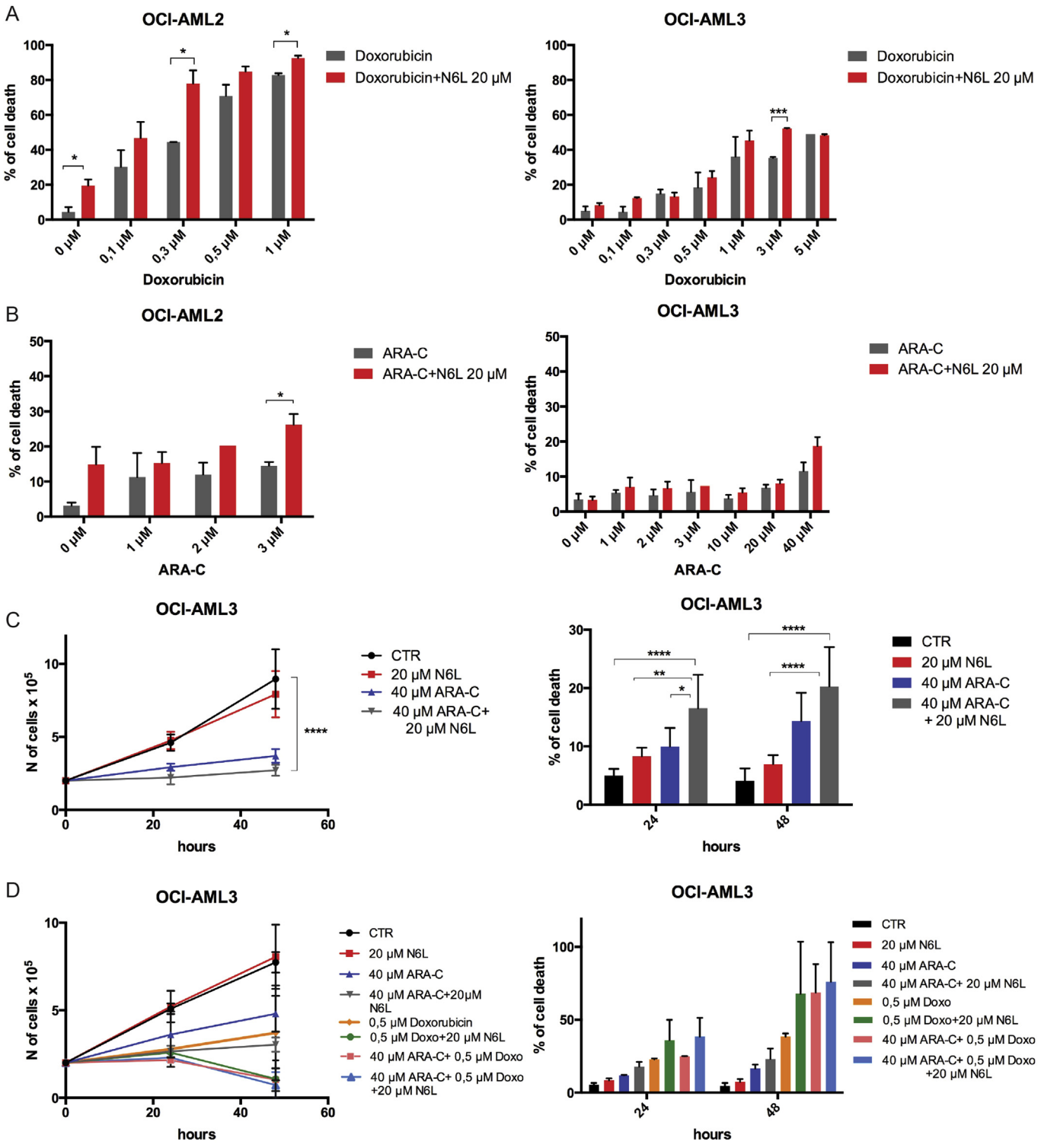

Fig. 6. (**A**) Percentage of cell death of OCI-AML2 and OCI-AML3 stained with Trypan Blue, treated or not with Doxorubicin at the indicated doses for 24 h; alone or in combination with 20 μM N6L. **(B)** Percentage of cell death of OCI-AML2 and OCI-AML3 analysed as described above, treated or not with cytarabine (ARA-C) at the indicated doses for 24 h; alone or in combination with 20 μM N6L. (**C**) Cell proliferation assay and percentage of cell death OCI-AML3 untreated (ctr) or treated with 20 μM of N6L or with 40 μM of ARA-C, or with the combination of two at the indicated time points (hours). Data represent mean ± SD of three different experiments, each performed in triplicate, analysed with Anova test with a p value **** < 0,0001. (**D**) Cell proliferation and percentage of cell death of OCI-AML3 untreated (ctr) or treated with N6L, ARA-C, doxorubicin alone or in combination at the indicated doses, from 24 to 48 h.

N6L dramatically reduces OCI-AML2 cell growth through activation of a p53 dependent apoptotic pathway. However, we also observed that N6L-triggered p53 activation in OCI-AML3 cells is weak, conferring resistance to N6L treatment within the 72 h time window. While p53 is wild-type in both cell lines, its initial levels as well as those of p14ARF and p21 are very low in OCI-AML3 with respect to OCI-AML2 cells [42]. This effect may be possibly ascribed to the delocalization and degradation of p14ARF played by NPM1c+

[25]. However it should be noted that a dose-dependent increase of p53, p21 and p14ARF is observable also in OCI-AML3 cells, which we ascribe to the ability of N6L to interact with NPM1c+ in the cytoplasm, thus protecting p14ARF from degradation. This was confirmed by the analysis of N6L cell shuttling. We found that N6L co-localizes with NPM1 and nucleolin in the nucleoli of OCI-AML2 cells, while a consistent fraction of N6L is observed in the cytosol of OCI-AML3 cells, where it co-localizes with NPM1c+.

We also found that the Thr199-phosphorylated form of NPM1 is present at higher basal levels in OCI-AML3 with respect to OCI-AML2 cells and that N6L treatment lead to its decrease but at a lesser extent in OCI-AML3 cells. Dephosphorylation at Thr199 has been reported to facilitate NPM1 activity in DNA repair [45]. However, whether the alteration of NPM1 phosphorylation plays an active role in N6L induced cell death requires further investigation.

Our data led us to hypothesize that, although a robust apoptotic response is not achievable in OCI-AML3 cells by N6L treatment alone, this drug might nevertheless sensitize cells harbouring NPM1c + to standard chemotherapy. First line treatment for AML consists in an induction therapy, which involves the administration of cytarabine plus an anthracycline drug (daunorubicin, doxorubicin or others), in the so-called 7 + 3 regimen [46], followed by a consolidation therapy or allogeneic stem cell transplantation. Therefore we resorted to test the effect of these drugs in our cell models. Similar with what observed with N6L, OCI-AML3 cells carrying NPM1c + resulted more resistant than OCI-AML2 to both doxorubicin and cytarabine treatment. However, we observed that N6L co-treatment with doxorubicin resulted in increasing the percentage of cell death. Similar synergic behavior was also observed in OCI-AML3 cells when N6L was administered together with cytarabine, reaching the higher effect at 48 h. Finally, a slight sensitization effect was also obtained in the triple combination, even though doxorubicin plus cytarabine were by themselves already highly toxic to OCI-AML3 cells.

Most adults with AML still die of their disease [46] and it is becoming increasingly evident that the 7 + 3 regimen is not enough to secure long term remission [46]. Moreover, the cardiotoxicity of anthracycline drugs prevents many patients from their prolonged use. For these reasons, variations of the 7 + 3 regimen ranging from dose intensification of either anthracyclines or cytarabine, the replacement of one of these agents with new ones or the incorporation of additional agents in standard 7 + 3, have been investigated by several clinical trials [47].

Our study suggest that N6L, a new agent that interferes with NPM1 protein-protein associations, and that has already completed Phase I/IIa clinical trials for different solid tumors, may be effective in treatment of AML with wild-type NPM1 and also, in combination with anthracycline and/or cytarabine, of AML with NPM1c+, which is the most common form of this disease.

Acknowledgements

This work was supported by a grant from Associazione Italiana Ricerca sul Cancro (IG2014-15197 to L.F.) and by grants of the University of Chieti “G. d’Annunzio” (Ateneo ex 60% to L.F.).

Appendix A. Supplementary data

Supplementary data related to this article can be found at https://doi.org/10.1016/j.canlet.2017.10.038.

Conflict of interest

The authors declare no conflict of interest.

References

[1] S. Grisendi, C. Mecucci, B. Falini, P.P. Pandolfi, Nucleophosmin and cancer, Nat. Rev. Cancer 6 (2006) 493–505.
[2] E. Emmott, J.A. Hiscox, Nucleolar targeting: the hub of the matter, EMBO Rep. 10 (2009) 231–238.
[3] E. Colombo, M. Alcalay, P.G. Pelicci, Nucleophosmin and its complex network: a possible therapeutic target in hematological diseases, Oncogene 30 (2011) 2595–2609.
[4] W. Wang, A. Budhu, M. Forgues, X.W. Wang, Temporal and spatial control of nucleophosmin by the Ran-Crm1 complex in centrosome duplication, Nat. Cell Biol. 7 (2005) 823–830.
[5] K. Murano, M. Okuwaki, M. Hisaoka, K. Nagata, Transcription regulation of the rRNA gene by a multifunctional nucleolar protein, B23/nucleophosmin, through its histone chaperone activity, Mol. Cell Biol. 28 (2008) 3114–3126.
[6] O. Ziv, A. Zeisel, N. Mirlas-Neisberg, U. Swain, R. Nevo, N. Ben-Chetrit, et al., Identification of novel DNA-damage tolerance genes reveals regulation of translesion DNA synthesis by nucleophosmin, Nat. Commun. 5 (2014), 5437.
[7] M. Okuwaki, K. Matsumoto, M. Tsujimoto, K. Nagata, Function of nucleophosmin/B23, a nucleolar acidic protein, as a histone chaperone, FEBS Lett. 506 (2001) 272–276.
[8] N. Feuerstein, P.K. Chan, J.J. Mond, Identification of numatrin, the nuclear matrix protein associated with induction of mitogenesis, as the nucleolar protein B23. Implication for the role of the nucleolus in early transduction of mitogenic signals, J. Biol. Chem. 263 (1988) 10608–10612.
[9] W.Y. Chan, Q.R. Liu, J. Borjigin, H. Busch, O.M. Rennert, L.A. Tease, et al., Characterization of the cDNA encoding human nucleophosmin and studies of its role in normal and abnormal growth, Biochemistry 28 (1989) 1033–1039.
[10] L. Léotoing, L. Meunier, M. Manin, C. Mauduit, M. Decaussin, G. Verrijdt, et al., Influence of nucleophosmin/B23 on DNA binding and transcriptional activity of the androgen receptor in prostate cancer cell, Oncogene 27 (2008) 2858–2867.
[11] J.P. Yun, J. Miao, G.G. Chen, Q.H. Tian, C.Q. Zhang, J. Xiang, et al., Increased expression of nucleophosmin/B23 in hepatocellular carcinoma and correlation with clinicopathological parameters, Br. J. Cancer 96 (2007) 477–484.
[12] A. Pianta, C. Puppin, A. Franzoni, D. Fabbro, C. Di Loreto, S. Bulotta, et al., Nucleophosmin is overexpressed in thyroid tumours, Biochem. Biophys. Res. Commun. 397 (2010) 499–504.
[13] Y. Nozawa, N. Van Belzen, A.C. Van der Made, W.N. Dinjens, F.T. Bosman, Expression of nucleophosmin/B23 in normal and neoplastic colorectal mucosa, J. Pathol. 178 (1996) 48–52.
[14] M. Tanaka, H. Sasaki, I. Kino, T. Sugimura, M. Terada, Genes preferentially expressed in embryo stomach are predominantly expressed in gastric cancer, Cancer Res. 52 (1992) 3372–3377.
[15] Y. Zhu, M. Shi, H. Chen, J. Gu, J. Zhang, B. Shen, et al., NPM1 activates metabolic changes by inhibiting FBP1 while promoting the tumourigenicity of pancreatic cancer cells, Oncotarget 6 (2015) 21443–21451, https://doi.org/10.18632/oncotarget.4167.
[16] J. Chen, J. Sun, L. Yang, Y. Yan, W. Shi, J. Shi, et al., Upregulation of B23 promotes tumour cell proliferation and predicts poor prognosis in glioma, Biochem. Biophys. Res. Commun. 466 (2015) 124–130.
[17] K. Holmberg Olausson, T. Elsir, K. Moazemi Goudarzi, M. Nistér, M.S. Lindström, NPM1 histone chaperone is upregulated in glioblastoma to promote cell survival and maintain nucleolar shape, Sci. Rep. 5 (2015), 16495.
[18] B. Falini, I. Nicoletti, N. Bolli, M.P. Martelli, A. Liso, P. Gorello, et al., Translocations and mutations involving the nucleophosmin (NPM1) gene in lymphomas and leukemias, Haematologica 92 (2007) 519–532.
[19] B. Falini, C. Mecucci, E. Tiacci, M. Alcalay, R. Rosati, L. Pasqualucci, et al., GIMEMA Acute Leukemia Working Party, Cytoplasmic nucleophosmin in acute myelogenous leukemia with a normal karyotype, N. Engl. J. Med. 352 (2005) 254–266.
[20] B. Falini, I. Nicoletti, M.F. Martelli, C. Mecucci, Acute myeloid leukemia carrying cytoplasmic/mutated nucleophosmin (NPMc? AML): biologic and clinical features, Blood 109 (2007) 874–885.
[21] B. Falini, N. Bolli, J. Shan, M.P. Martelli, A. Liso, A. Pucciarini, et al., Both carboxy-terminus NES motif and mutated tryptophan(s) are crucial for aberrant nuclear export of nucleophosmin leukemic mutants in NPMc+ AML, Blood 107 (2006) 4514–4523.
[22] A. Gallo, C. Lo Sterzo, M. Mori, A. Di Matteo, I. Bertini, L. Banci, et al., Structure of nucleophosmin DNA-binding domain and analysis of its complex with a G-quadruplex sequence from the c-MYC promoter, J. Biol. Chem. 287 (2012) 26539–26548.
[23] S. Chiarella, A. De Cola, G.L. Scaglione, E. Carletti, V. Graziano, D. Barcaroli, et al., Nucleophosmin mutations alter its nucleolar localization by impairing G-quadruplex binding at ribosomal DNA, Nucleic Acids Res. 41 (2013) 3228–3239.
[24] L. Federici, B. Falini, Nucleophosmin mutations in acute myeloid leukemia: a tale of protein unfolding and mislocalization, Protein Sci. 22 (2013) 545–556.
[25] E. Colombo, P. Martinelli, R. Zamponi, D.C. Shing, P. Bonetti, L. Luzi, et al., Delocalization and destabilization of the Arf tumour suppressor by the leukemia-associated NPM mutant, Cancer Res. 66 (2006) 3044–3050.
[26] P. Bonetti, T. Davoli, C. Sironi, B. Amati, P.G. Pelicci, E. Colombo, Nucleophosmin and its AML-associated mutant regulate c-Myc turnover through Fbw7 gamma, J. Cell Biol. 182 (2008) 19–26.

[27] N.I. Noguera, M.S. Song, M. Divona, G. Catalano, K.L. Calvo, F. García, et al., Nucleophosmin/B26 regulates PTEN through interaction with HAUSP in acute myeloid leukemia, Leukemia 27 (2013) 1037–1043.
[28] B. Falini, I. Gionfriddo, F. Cecchetti, S. Ballanti, V. Pettirossi, M.P. Martelli, Acute Myeloid Leukemia with mutated nucleophosmin (NPM1): any hope for a targeted therapy? Blood Rev. 25 (2011) 247–254.
[29] A. Di Matteo, M. Franceschini, S. Chiarella, S. Rocchio, C. Travaglini-Allocatelli, L. Federici, Molecules that target nucleophosmin for cancer treatment: an update, Oncotarget 7 (2016) 44821–44840.
[30] D. Destouches, N. Page, Y. Hamma-Kourbali, V. Machi, O. Chaloin, S. Frechault, et al., A simple approach to cancer therapy afforded by multivalent pseudopeptides that target cell-surface nucleoproteins, Cancer Res. 71 (2011) 3296–3305.
[31] D. Destouches, E. Huet, M. Sader, S. Frechault, G. Carpentier, F. Ayoul, et al., Multivalent pseudopeptides targeting cell surface nucleoproteins inhibit cancer cell invasion through tissue inhibitor of metalloproteinases 3 (TIMP-3) release, J. Biol. Chem. 287 (2012) 43685–43693.
[32] C. Birmpas, J.P. Briand, J. Courty, P. Katsoris, Nucleolin mediates the anti-angiogenesis effect of the pseudopeptide N6L, BMC Cell Biol. 13 (2012) 32.
[33] S. Kossatz, J. Grandke, P. Couleaud, A. Latorre, A. Aires, K. Crosbie-Staunton, et al., Efficient treatment of breast cancer xenografts with multifunctionalized iron oxide nanoparticles combining magnetic hyperthermia and anti-cancer drug delivery, Breast Cancer Res. 17 (2015) 66.
[34] E. Benedetti, A. Antonosante, M. d'Angelo, L. Cristiano, R. Galzio, D. Destouches, et al., Nucleolin antagonist triggers autophagic cell death in human glioblastoma primary cells and decreased in vivo tumor growth in orthotopic brain tumor model, Oncotarget 6 (39) (2015) 42091–42104.
[35] D. Destouches, M. Sader, S. Terry, C. Marchand, P. Maillé, P. Soyeux, et al., Implication of NPM1 phosphorylation and preclinical evaluation of the nucleoprotein antagonist N6L in prostate cancer, Oncotarget 7 (43) (2016).
[36] M.E. Gilles, F. Maione, M. Cossutta, G. Carpentier, L. Caruana, S. Di Maria, et al., Nucleolin targeting impairs the progression of pancreatic cancer and promotes the normalization of tumor vasculature, Cancer Res. 76 (24) (2016) 7181–7193.
[37] D.M. Mitrea, C.R. Grace, M. Buljan, M.K. Yun, N.J. Pytel, J. Satumba, et al., Structural polymorphism in the N-terminal oligomerization domain of NPM1, Proc. Natl. Acad. Sci. U. S. A. 111 (2014) 4466–4471.
[38] A. Di Matteo, M. Franceschini, A. Paiardini, A. Grottesi, S. Chiarella, S. Rocchio, et al., Structural investigation of nucleophosmin interaction with the tumor suppressor Fbw7γ, Oncogenesis 6 (9) (2017) e379, https://doi.org/10.1038/oncsis.2017.78.
[39] M.S. Scott, P.V. Troshin, G.J. Barton, NoD: a Nucleolar localization sequence detector for eukaryotic and viral proteins, BMC Bioinforma. 12 (2011) 317.
[40] H. Quentmeier, M.P. Martelli, W.G. Dirks, N. Bolli, A. Liso, R.A. Macleod, et al., Cell line OCI/AML3 bears exon-12 NPM gene mutation-A and cytoplasmic expression of nucleophosmin, Leukemia 19 (10) (2005) 1760–1767.
[41] L. Federici, A. Arcovito, G.L. Scaglione, F. Scaloni, C. Lo Sterzo, A. Di Matteo, et al., Nucleophosmin C-terminal leukemia-associated domain interacts with G-rich quadruplex forming DNA, J. Biol. Chem. 285 (2010) 37138–37149.
[42] A. De Cola, L. Pietrangelo, F. Forlì, D. Barcaroli, M.C. Budani, V. Graziano, et al., AML cells carrying NPM1 mutation are resistant to nucleophosmin displacement from nucleoli caused by the G-quadruplex ligand TmPyP4, Cell Death Dis. 5 (2014) e1427.
[43] F. Scaloni, L. Federici, M. Brunori, S. Gianni, Deciphering the folding transition state structure and denatured state properties of Nucleophosmin C-terminal domain, Proc. Natl. Acad. Sci. U. S. A. 107 (2010) 5447–5452.
[44] S.M. Leong, B.X. Tan, B. Bte Ahmad, T. Yan, L.Y. Chee, S.T. Ang, et al., Mutant nucleophosmin deregulates cell death and myeloid differentiation through excessive caspase-6 and -8 inhibition, Blood 116 (2010) 3286–3296.
[45] C.Y. Lin, B.C. Tan, H. Liu, C.J. Shih, K.Y. Chien, C.L. Lin, et al., Dephosphorylation of nucleophosmin by PP1β facilitates pRB binding and consequent E2F1-dependent DNA repair, Mol. Biol. Cell 21 (24) (2010) 4409–4417.
[46] G.J. Roboz, Current treatment of acute myeloid leukemia, Curr. Opin. Oncol. 24 (2012) 711–719.
[47] A. Tefferi, L. Letendre, Going beyond 7 + 3 regimens in the treatment of adult acute myeloid leukemia, J. Clin. Oncol. 30 (20) (2012 Jul 10) 2425–2428.